Arch. Metall. Mater. **70** (2025), 4, 1937-1944

DOI: https://doi.org/10.24425/amm.2025.156280

F. BAIRA[1*], Y. ACHOUR[2,3], Y. BENKRIMA[4], S. ZIDANI[5], K. BAIRA[1], R. OUACHE[1], Y. MEGDOUD[6], T.A. CHINAR[1], M. TAMERABET[1]

ELECTRONIC, MAGNETIC, AND ELASTIC PROPERTIES OF $FeNi_3$ AND $FeNi_2Pt$

The ab initio pseudopotential method relies on Density Functional Theory (DFT), utilizing the generalized gradient approximation (GGA) as outlined by Perdew-Burke-Ernzerhof (PBE). Implemented through the Siesta program, this method examines the structural and optical properties of the nickel-iron alloy (Fe-Ni) that crystallizes in the $FeNi_3$ structure. This approach is highly regarded for its accuracy in predicting the crystal structure and properties of $FeNi_3$. The computed structural parameters align closely with both theoretical and experimental data, confirming the reliability of these predictions. The lattice constants, calculated at zero pressure, match previously reported theoretical and experimental results. Furthermore, the computed properties, including the Band Structure, Total Density of States (DOS), and Partial Density of States (PDOS), and elastic constants values for the alloy, suggesting its suitability for specific applications in targeted fields.

Keywords: DFT; $FeNi_2Pt$; Electronic Properties; Elastic Properties

1. Introduction

The interest that has persisted since the late 20th century until now is focused on the study of numerous metallic materials and alloys, particularly iron and its alloys such as iron-nickel (Fe-Ni) alloys, specifically the $FeNi_3$ compound. These alloys have garnered significant attention and extensive study due to their extensive utilization in various advanced and sensitive applications, owing to their notable properties, which include:

Superconductivity, optical conductivity, high magnetic permeability, high saturation magnetization, high Curie temperature, near-zero magnetostriction, variable magnetoresistance, low coercivity, corrosion resistance, low energy losses, and very low coefficient of thermal expansion.

Fe-Ni alloys have been known for a long time and have been utilized in various industrial applications that require high saturation magnetization and low coercive field. Additionally, their structural and chemical properties, which play a crucial role in determining their magnetic characteristics, have been relied upon, leading to their adoption and utilization in certain industrial applications such as electromagnetic wave absorption, antennas, magnetic sensors, magnetic resonance imaging devices, catalysts, magnetic recording heads, sensors, pharmaceutical and pharmaceutical product manufacturing, and other applications [1-7].

The electrical properties of NiFe thin films rely strongly on the composition and processing control [8].Tang et al. [9] reported that film resistivity showed an approximately linear relationship with surface roughness, The reduction in surface roughness should lead to a decrease in the film resistivity. Choe and Steinback [10] reported the effect of surface roughness on magnetoresistance and magnetic properties of NiFe films. The thermal mechanical characteristic development of NiFe thin film is an important issue for material applications. Bruckner et al. [11] reported the densification by atomic rearrangement in grain-boundaries (from room temperature to 250°C and abnormal grain growth (especially between 300 and 400 °C may be the reason for the generation of tensile stress in NiFe films.

According to the aforementioned concerning the importance of the $FeNi_3$ compound in the manufacturing of various modern sensitive applications and its excellent properties, as well as previous studies that investigated its different electronic,

[1] UNIVERSITY OF BATNA 2, FACULTY OF TECHNOLOGY, DEPARTMENT OF SCIENCES AND TECHNOLOGY, ALLEYS 53, CONSTANTINE AVENUE. FÉSDIS, BATNA 05078, ALGERIA
[2] UNIVERSITÉ AMAR THELIDJI DE LAGHOUAT, LABORATOIRE DE PHYSIQUE DES MATÉRIAUX (LPM), BP37G, ROUTE DE GHARDAÏA, 03000 LAGHOUAT, ALGERIA
[3] ECOLE NORMALE SUPÉRIEURE DE LAGHOUAT, BP 4033 RUE DES MARTYRS, LA GARE, 03000 LAGHOUAT, ALGERIA
[4] ECOLE NORMALE SUPÉRIEURE DE OUARGLA, 30000 OUARGLA, ALGERIA
[5] UNIVERSITY OF BATNA DEPARTEMENT OF FOOD TECHNOLOGY, LABORATORY OF FOOD SCIENCE (LSA), INSTITUTE OF VETERINARY AND AGRICULTURAL SCIENCES, 1 HADJ LAKHDAR, ALLEYS MAY 19 BISKRA AVENUE, BATNA, 05000, ALGERIA
[6] CENTRE UNIVERSITY MORSLI ABDALLAH TIPAZA, INSTITUTE OF SCIENCES, ALGERIA
* Correspondinh author: f.baira@univ-batna2.dz; b-amina1@hotmail.fr

magnetic, and elastic properties using experimental and theoretical approaches, the aim of this work was to study these physical properties using a different method that has not been employed in previous studies, namely Density Functional Theory (DFT) within the SIESTA simulation program. Therefore, this study serves as an addition to compare our results with previous findings.

Furthermore, we are also investigating the same physical properties of the $FeNi_2Pt$ compound to determine the impact of substituting a Ni atom with a Pt atom in the structure of $FeNi_3$. This is achieved by comparing the obtained results for the two studied compounds, $FeNi_3$ and $FeNi_2Pt$. It is worth mentioning that previous works on the $FeNi_3$ compound have investigated it with the addition of other elements apart from platinum (Pt).

In this study, we highlighted the importance of replacing the nickel atom (Ni) with a platinum atom (Pt), and discovering the new properties that the compound $FeNi_2Pt$ now has, which are completely different from what was achieved in the $FeNi_3$ compound.

2. Methodology

In this work, the electronic, magnetic, and elastic properties of the $FeNi_3$ and $FeNi_2Pt$ compounds were studied and calculated using Density Functional Theory (DFT), implemented in the Spanish Initiative for Electronic Simulations (SIESTA) program [12]. The obtained results were compared to shed light on the impact of platinum as a dopant on the mentioned properties of the original compound. Our calculations were conducted based on the following choices:

The calculations were performed using the Troullier-Martins non-local pseudopotential method with a norm-conserving criterion. The convergence criterion for the total energy was set to 10^{-4} atomic units (a.u.), and the energy shift was chosen as 80 meV. The mesh cutoff energy (E_Cut) for the simulation was set to 400 eV.

A double-zeta polarized (DZP) basis set with polarized orbitals for Fe and Ni atoms was employed in the simulation program. The compound was placed in a supercell during the simulation, allowing for an extended system size.

The conjugate gradient method was utilized to calculate the Hellmann-Feynman forces applied to the atoms. All forces after structural relaxation were required to be less than 10^{-3} eV/Å. The maximum tolerance for ion displacement was set to 0.05 Å. These parameters ensured accurate and reliable calculations of the physical properties of the studied compounds. After specifying these parameters, the $FeNi_3$ crystalline lattice with a face-centered cubic (FCC) structure was chosen, and one Ni atom was replaced with a Pt atom, resulting in the $FeNi_2Pt$ compound.

3. Results and discussion

The $FeNi_3$ compound possesses diverse and significant physical properties as mentioned in the general introduction. Therefore, it is highly intriguing to study these properties using various theoretical and experimental methods in order to extract and compare the results, aiming to understand their reliance and utilization in different mentioned industrial applications.

In fact, previous works [13,14] have shown that the hysteresis cycle of this compound undergoes changes in its shape when compared to its pristine state. Additionally, $FeNi_3$ particles are widely employed as solid catalysts in dye-sensitive solar cells (DSSCs), where they are compared to Pt catalysts [15].

3.1. Electronic properties

In this work, we focus on presenting and discussing the band structure and the total density of states (DOS) with the determination of the contributions of each atom's electronic orbitals to the energy range, i.e., the partial density of states (PDOS).

3.1.1. Band structure

In the SIESTA program, we employed the GGA (Generalized Gradient Approximation) approximation to calculate the band structures of the $FeNi_3$ and $FeNi_2Pt$ compounds, taking into account electronic spin.

Figs. 1 and 2 illustrate the band structures of the $FeNi_3$ and $FeNi_2Pt$ compounds, respectively.

From Figs. 1 and 2, it is evident that there is an overlap of the upper valence band peaks with the lower conduction band valleys, indicating the metallic nature of the compounds. The results also demonstrate a significant impact of platinum doping on the electronic structure of the emerging compound $FeNi_2Pt$. This effect is manifested in the appearance of new energy levels in the structure of $FeNi_2Pt$ that were not available for electrons in the original compound $FeNi_3$ near the Fermi level. It is apparent that platinum doping increases the energy band dispersion in the immediate vicinity of the Fermi level, resulting in a sharp and rapid curvature of the available electron energy states due to changes in their kinetic momentum, particularly at the high-symmetry

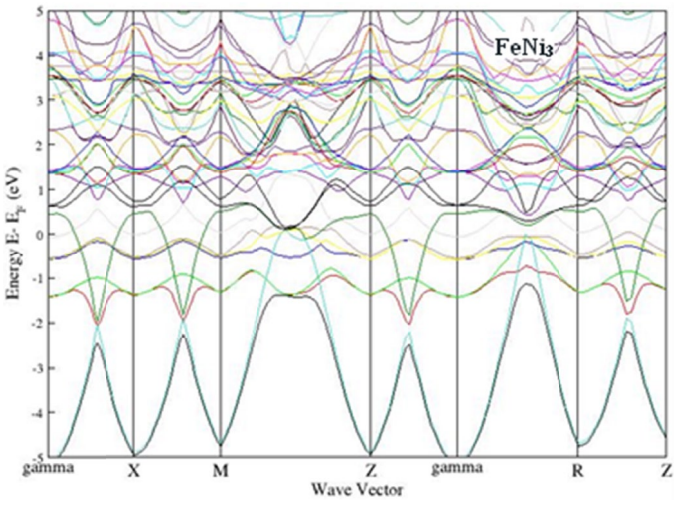

Fig. 1. Band structure of the $FeNi_2Pt$

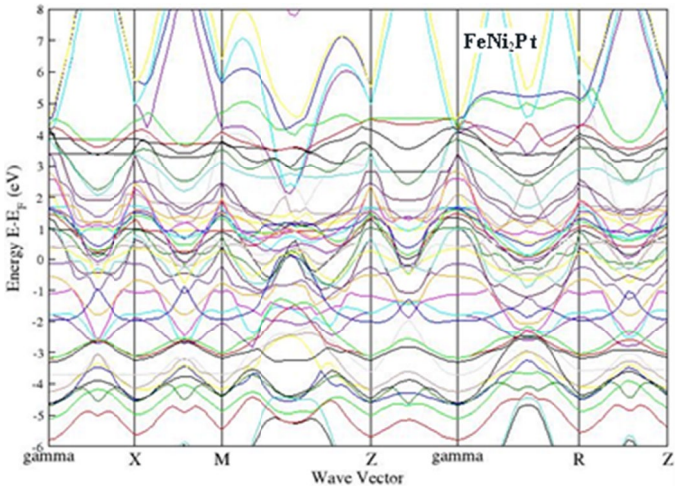

Fig. 2. Band structure of the $FeNi_2Pt$

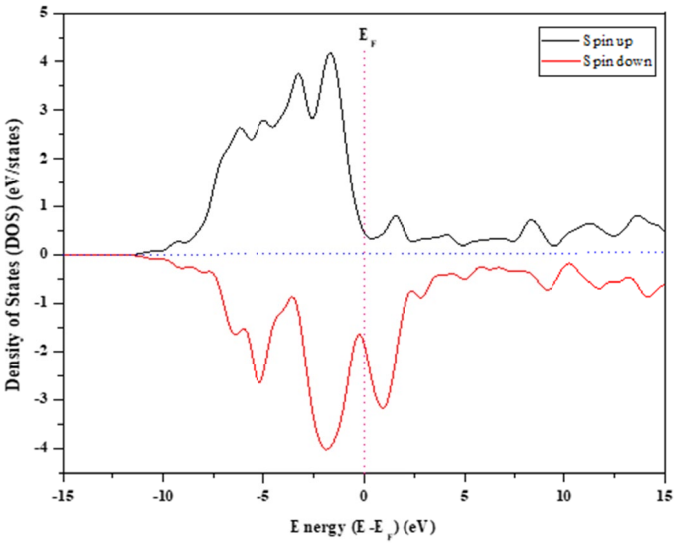

Fig. 3. Total Density of States (DOS) for the $FeNi_3$

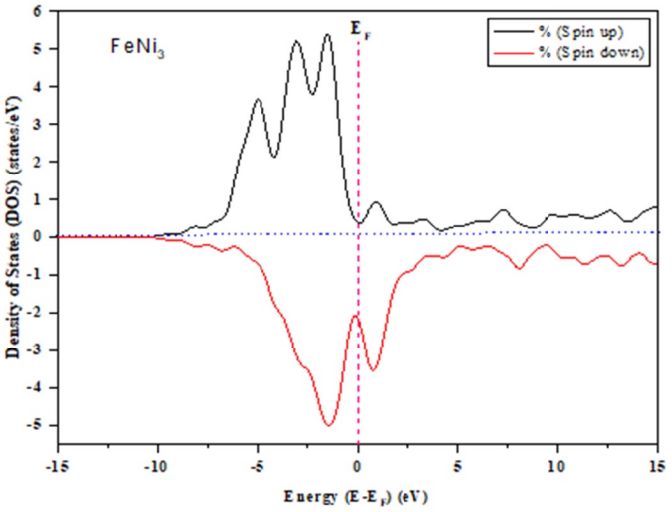

Fig. 4. Total Density of States (DOS) for the $FeNi_2Pt$

points of the first Brillouin zone. Therefore, we can conclude that this doping has a positive effect on the mobility of carrier electrons, which can enhance the electrical conductivity of the $FeNi_2Pt$ compound compared to its undoped counterpart $FeNi_3$.

3.1.2. Total Density of States (DOS)

The simulation results, within the generalized approximation for exchange and correlation energy, reveal that the magnetic symmetry in the crystalline structure of the studied compounds leads to distinct group-theoretical symmetries. The effect of this symmetry is manifested in the distortion of the electronic density of states for the highest and lowest electronic spin states, indicating their contrasting magnetic properties.

We analyze the total density of states for the $FeNi_3$ and $FeNi_2Pt$ compounds to understand the origin of the states forming the valence and conduction bands and to comprehend the interactions between the atoms in the studied compounds.

Figs. 3 and 4 illustrate the total density of states for the $FeNi_3$ and $FeNi_2Pt$ compounds, respectively.

From Figs. 3 and 4, it is observed that the total density of states (DOS) for both $FeNi_3$ and $FeNi_2Pt$ compounds exhibits non-symmetric behavior for the highest and lowest electron spin states, indicating their acquired magnetic properties as mentioned earlier. Additionally, the density of states for the highest and lowest electron spin states in the valence band region, ranging from –7 eV to the Fermi level, is higher than their counterparts in the conduction band region, ranging from the Fermi level to +5 eV. Furthermore, the total DOS calculated for $FeNi_3$ and $FeNi_2Pt$ compounds is high in the vicinity of the Fermi level.

In the valence band region of the $FeNi_2Pt$ compound, the energy band width is larger than that of the $FeNi_3$ compound in the same region, indicating a higher electron population in the valence band. Near the Fermi level, the $FeNi_2Pt$ compound exhibits a higher peak density of states in the higher and lower spin states, with values of 4.2 states/eV and 5.42 states/eV (higher spin) and 5.01 states/eV (lower spin) for $FeNi_3$ compound. At the Fermi level, the density of states shows small values for the higher spin state, with 0.37 states/eV for both compounds, while for the lower spin state, it takes the values of –1.8 states/eV for $FeNi_2Pt$ and –2.19 states/eV for $FeNi_3$. These observations indicate that both compounds exhibit semi-metallic behavior, possessing both metallic and semi-conducting characteristics.

Moreover, both compounds exhibit ferromagnetic properties, with magnetic moments of 5.20 μB and 5.071 μB for $FeNi_3$ and $FeNi_2Pt$, respectively. Therefore, $FeNi_3$ and $FeNi_2Pt$ can be considered as soft ferromagnetic materials, demonstrating excellent properties for directing and conducting magnetic flux. They could find applications in various fields where there is a need for directing and converting magnetic energy, such as transformers, magnetic valves, sensors, and electric motors. It is worth noting that this type of material has a high magnetic scaling ability, allowing for high magnetic strength in small volumes. Additionally, their low magnetic saturation makes them highly responsive to external magnetic fields.

3.1.3. Partial Density of States (PDOS)

Partial Density of States (PDOS) enables the investigation of the role of electrons in different atomic valence orbitals and their impact on electronic properties, particularly polarization. In this study, the PDOS was calculated using the GGA approximation for the compounds $FeNi_3$ and $FeNi_2Pt$, and analyzed to understand the electron behavior near the Fermi level.

Fig. 5 illustrates the PDOS for the $FeNi_3$ compound, calculated for the 3d atomic valence electrons of the Fe element represented by the black (spin-up) and red (spin-down) lines, and the 3d atomic valence electrons of the Ni element represented by the green (spin-up) and blue (spin-down) lines. The vertical dotted line represents the position of the Fermi level.

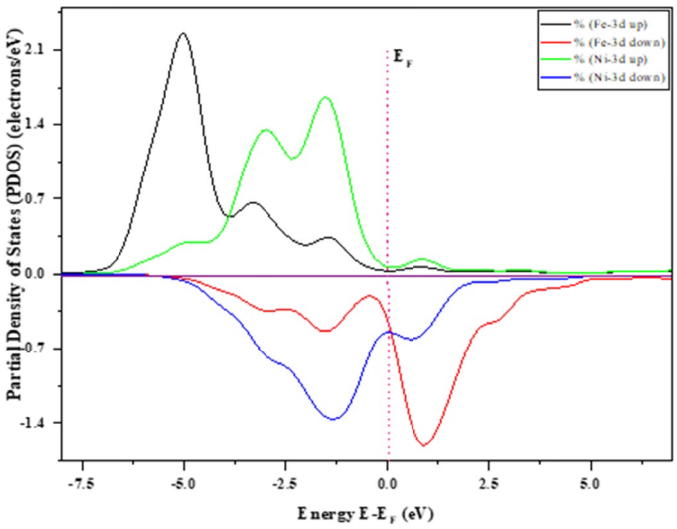

Fig. 5. The Partial Density of States (PDOS) shows the contribution of the atomic level (3d) for the Fe and Ni atoms in the $FeNi_3$

In Fig. 6, The PDOS illustrates the density for the $FeNi_3$ compound, calculated for the atomic levels (3d and s4) of both Fe and Ni elements, in order to determine which levels, contribute the most.

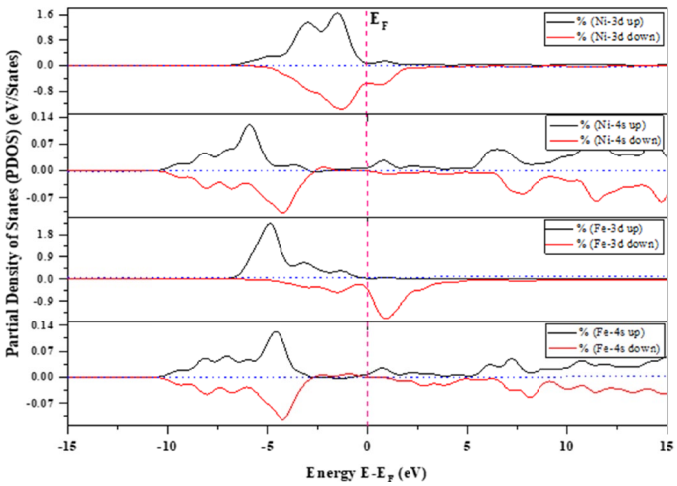

Fig. 6. The Partial Density of States (PDOS) reveals the contribution of the atomic levels (3d and 4s) of the Fe and Ni atoms

Fig. 7, the PDOS demonstrates the density for the $FeNi_2Pt$ compound, calculated for the atomic level 3d of the Fe element represented by the black (spin-up) and red (spin-down) lines, the atomic level 3d of the Ni element represented by the green (spin-up) and blue (spin-down) lines, and the atomic level 5d of the Pt element represented by the light blue (spin-up) and pink (spin-down) lines. The vertical dotted line in red indicates the position of the Fermi level.

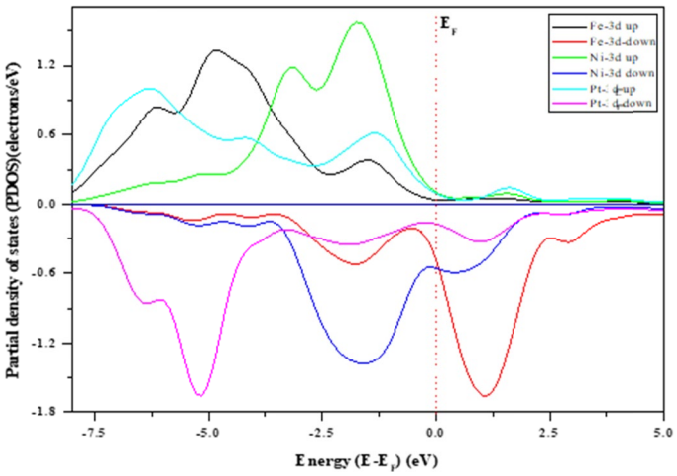

Fig. 7. The Partial Density of States (PDOS) illustrates the contribution of the 3d atomic level for both Fe and Ni atoms, as well as the 5d atomic level for the Pt atom, in the $FeNi_2Pt$ compound

Fig. 8, the PDOS reveals the density for the $FeNi_2Pt$ compound, calculated for the atomic levels 3d and 4s of both Fe and Ni elements, and the atomic levels 5d and 6s of the Pt element, in order to determine which levels contribute the most.

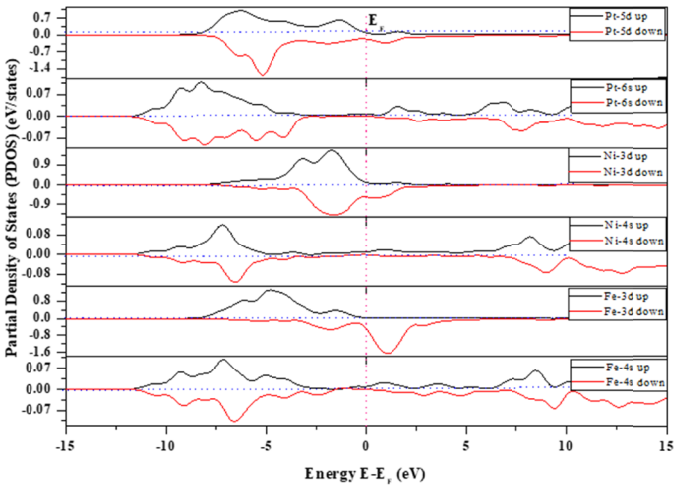

Fig. 8. The Partial Density of States (PDOS) illustrates the contribution of the 3d and 4s atomic levels for both Fe and Ni atoms, as well as the 5d and 6s atomic levels for the Pt atom, in the $FeNi_2Pt$

Based on the different distributions of electron spin states (spin up and spin down), the electron spin polarization is determined. Starting from a single unit cell, this polarization is then generalized to all atomic domains to assess the contributions of

iron (Fe), nickel (Ni), and platinum (Pt) atoms in the $FeNi_3$ and $FeNi_2Pt$ compounds. We have calculated the expected density of states along the electron energy bands (E-E_F). From the partial density of states (PDOS) distributions, as depicted in the previous figures related to PDOS, it can be observed that the electronic states primarily reside within the active region bounded by [+4.5eV, –6.7eV] relative to the Fermi levels for the $FeNi_3$ compound, and [+4.5eV, –7.5eV] relative to the Fermi levels for the $FeNi_2Pt$ compound. Furthermore, a slight deviation from the Fermi level can be noticed.

As for the $FeNi_3$ compound, extremely small values of state density are observed for the spin-up state, with a value of 0.06 states/eV for the nickel (Ni) element and 0.03 states/eV for the iron (Fe) element. In the spin-down state, the density takes a value of 0.54 states/eV for the nickel (Ni) element and 0.48 states/eV for the iron (Fe) element. The contribution of the atomic level (3d) for the iron element is relatively lower compared to the atomic level (3d) for the nickel element, with slight contributions close to zero for the orbital electrons (S4) in both atoms.

Concerning the $FeNi_2Pt$ compound, a near absence of state density is observed in the spin-up state for all elements. In the spin-down state, the density takes a value of 0.5 states/eV for the iron (Fe) element, 0.6 states/eV for the nickel (Ni) element, and 0.2 states/eV for the platinum (Pt) element.

These results confirm that both studied compounds exhibit a semi-metallic characteristic.

3.2. Elasticity properties

The mechanical properties of crystals are determined when they are subjected to external forces such as tension, compression, shear, or bending, which lead to changes in their shape and, in some cases, to fracture or collapse.

One of the essential properties of the ground state of solid materials is elasticity properties, as they provide information about heat capacity, external pressure, Debye temperature, and help determine the nature of bonds between adjacent atomic levels, as well as the hardness and flexibility of materials.

3.2.1. Elastic constants

Elastic constants, denoted as C_{ij} (Modulus of Elasticity), represent the ability of a material to regain its original shape after the removal of the applied force causing deformation. There are different types of these constants, which depend on the type of deformation the material undergoes, such as elongation, bending, and others. They are represented by the ratio of the applied stress σ to the resulting strain ε and can be expressed using one of the following formulas [16]:

$$\begin{cases} \sigma_i = C_{ij}\varepsilon_j \\ \varepsilon_i = S_{ij}\sigma_j \end{cases} \quad i, j = 1,2,3,4,5,6 \tag{1}$$

Where C_{ij} represents the extension of the hardness constants (Tensor of hardness constants) and S_{ij} represents the extension of the elastic constants (Tensor of elastic constants), also known as the compliance tensor, which is the inverse of the hardness tensor. The significance of these tensors lies in the fact that they precisely describe the elastic properties of solid materials and govern the forces underlying deformations. For the cubic system, the hardness coefficients are determined through nine independent elastic constants [16,17]. In the cubic system, it is sufficient to calculate the following elastic constants: C_{11}, C_{12}, C_{44}.

TABLE 1 presents the calculated values of the coefficients C_{11}, C_{12}, C_{44} for the compounds $FeNi_3$ and $FeNi_2Pt$, along with a comparison to previous theoretical and experimental results.

TABLE 1

Calculated values of the coefficients C_{11}, C_{12}, C_{44} for the compounds $FeNi_3$ and $FeNi_2Pt$

C_{44} (GPa)	C_{12} (GPa)	C_{11} (GPa)	Results	The compound
127.909	156.027	259.358	The result of our work	$FeNi_3$
124.078	153.705	273.534	Theoretical result [16]	
122.8	155.7	233.7	Theoretical result [17]	
119.2	144.4	230.4	Experimental result [18]	
114.7	136.9	237.2	Theoretical result [19]	
145.9	160.4	260.2	Theoretical result [20]	
146.7	168.9	243.2	Theoretical result [20]	
108.4	150.8	287.1	Theoretical result [21]	
127.908	156.029	259.361	Theresult of our work	$FeNi_2Pt$

We observe in the table above the recorded results are very close and similar to previous theoretical and experimental results. Additionally, the cubic elastic constants $C_{11} = C_{22} = C_{33}$ are high, indicating high resistance to axial compression in these directions. The shear elastic constants $C_{44} = C_{55} = C_{66}$ are lower than the other constant values, indicating lower shear in these directions. It is also noteworthy that all the elastic constants are positive and satisfy the stability condition for the compounds $FeNi_3$ and $FeNi_2Pt$, as governed by the following stability criterion specific to the cubic system [22-26]:

$$\begin{cases} C_{11} - C_{12} > 0 \\ C_{44} > 0 \\ C_{11} + 2C_{12} > 0 \end{cases} \tag{2}$$

3.2.2. Elastic moduli

Using the calculated values of the elastic constants C_{11}, C_{12}, C_{44} for the compounds $FeNi_3$ and $FeNi_2Pt$, various elastic moduli were determined to assess the hardness and brittleness of the compounds. The following elastic moduli were calculated: bulk modulus B, shear modulus G, Young's modulus E, Lamé's moduli λ and μ. To measure hardness, the B/G ratio was calculated. Additionally, the Poisson's ratio ν was determined to characterize the bond type between the atoms in the studied compounds.

The bulk modulus B is calculated using the Hill approximation [27,29] as follows:

$$B_H = \frac{(C_{11} + 2C_{12})}{3} \tag{3}$$

The shear modulus G is calculated using the Hill approximation [23,24] as follows:

$$G_H = \frac{1}{2}\left[\frac{(C_{11} - C_{12} + 3C_{44})}{5} + \frac{5(C_{11} - C_{12})C_{44}}{\left[4C_{44} + 3(C_{11} - C_{12})\right]}\right] \tag{4}$$

The Young's modulus E is calculated using the Hill approximation [23,24] as follows:

$$E_H = 2G(1 + \nu) \tag{5}$$

The Lamé's moduli μ and λ are calculated as follows:

$$\mu = \frac{E}{\left[2(1+\nu)\right]} \tag{6}$$

$$\lambda = \frac{\nu E}{\left[(1+\nu)(1-2\nu)\right]} \tag{7}$$

To determine the type of bonding between adjacent atomic planes, we calculate the Poisson's ratio ν using the Hill approximation [27,28]:

$$\nu_H = \frac{(3B - 2G)}{(2G + 6B)} \tag{8}$$

If the Poisson's ratio ν is less than the value of 0.1 ($\nu < 0.1$), the bonding between atoms is considered to be covalent. However, for most known solid materials such as metals, polymers, and ceramics, the bonding is predominantly ionic, and the value of the Poisson's ratio [29,30] is as follows:

$$0.25 < \nu < 0.35 \tag{9}$$

The B/G ratio, calculated from the compressional modulus B and shear modulus G, is theoretically correlated with the Poisson's ratio, which takes values of $\nu > 0.26$ when the B/G ratio exceeds 1.75. This relationship is also supported by the empirical criterion proposed by Pugh [27,28] for material hardness or brittleness. According to this criterion, materials are classified as ductile when the B/G ratio exceeds 1.75, while materials with a B/G ratio below 1.75 are considered brittle and prone to rapid fracture.

TABLE 2 illustrates the results of calculating the elastic moduli for the compounds $FeNi_3$ and $FeNi_2Pt$, along with a comparison to previous theoretical and experimental findings specifically for the $FeNi_3$ compound.

Based on the results of the density analysis near the Fermi level, it can be inferred that there is strong hybridization between the 3d atomic orbitals of nickel (Ni) and iron (Fe) atoms. Nickel (Ni) exhibits superior conductivity due to its higher values of the density of states compared to iron (Fe) in both $FeNi_3$ and $FeNi_2Pt$ compounds. In the case of the $FeNi_2Pt$ compound, there is a significant contribution from the 5d atomic orbitals of platinum (Pt), which increases the electronic density of states in the valence region, making it a more magnetic compound. The substantial contribution of the (d) atomic orbitals to the high electronic density occurs near the Fermi level, indicating the chemical and thermal activity of these compounds, consistent with previous findings.

By calculating the elastic properties, including the elastic constants and moduli, it is evident that the results for the $FeNi_3$ compound closely align with previous theoretical and experimental studies. The $FeNi_3$ and $FeNi_2Pt$ compounds exhibit similar values, suggesting that the doping does not significantly affect the elastic properties of the original compound. Additionally, both compounds, $FeNi_3$ and $FeNi_2Pt$, demonstrate high values for the compressional modulus (B), shear modulus (G), Young's modulus (E), as well as high values for the Lamé parameters (μ and λ). Furthermore, the calculated B/G ratio of 2.142 (>1.75) indicates that these compounds possess high hardness. The Poisson's ratio ($\nu \approx 0.3$) indicates that the bonding between atoms is ionic rather than covalent.

4. Conclusion

Based on the mentioned approach in the calculation method, and relying on ab-initio principles, the electronic, elastic, and magnetic properties of $FeNi_3$ and $FeNi_2Pt$ compounds were investigated. By comparing the results obtained through the generalized gradient approximation (GGA), the following conclusions can be drawn:

TABLE 2

Results of elastic modulus calculations for the compounds $FeNi_3$ and $FeNi_2Pt$

μ	λ	B/G	ν	E (GPa)	B (GPa)	G_H (GPa)	Results	
88.922	**131.190**	2.142	0.298	230.842	190.471	**88.921**	The result of our work	**$FeNi_3$**
93.753	131.614	2.065	0.292	242.257	193.648	**93.789**	Theory [16]	
77.663	129.88	2.340	0.313	203.926	181.7	**77.660**	Theory [17]	
79.237	120.252	2.184	0.3014	206.238	173.066	**79.237**	Experimental [18]	
82.294	115.528	2.070	0.292	212.647	170.333	**82.298**	Theory [19]	
94.994	130.110	2.039	0.289	244.894	193.666	**94.975**	Theory [20] Ferromagnetic	
85.118	136.544	2.276	0.308	222.669	193.666	**85.094**	Theory [20] Paramagnetic	
90.00	136.130	2.181	0.301	234.179	196.233	**89.993**	Theory [21]	
88.922	**131.192**	2.142	0.298	230.842	190.474	**88.921**	The result of our work	$FeNi_2Pt$

– The calculation of electronic properties reveals that platinum doping leads to an increase in electrical conductivity and improvement in the resulting compound $FeNi_2Pt$ compared to $FeNi_3$. This aspect facilitates the design of electronic devices with specific functions, such as transistors, diodes, and high-density storage disk readers.
– It is also inferred that the studied compounds belong to the category of semi-metallic materials, possessing both metallic and semi-conducting characteristics.

Furthermore, it can be concluded that the magnetic symmetry in the crystal structure of the studied compounds results in a distortion of the electronic density of states of the higher and lower spin-up and spin-down electron states, indicating their contrasting magnetic properties. $FeNi_2Pt$ is considered superior in terms of its ferromagnetic property. $FeNi_3$ and $FeNi_2Pt$ can be regarded as good soft ferromagnetic materials, exhibiting excellent properties in directing and conducting magnetic flux. They are potential candidates for various applications that require the manipulation and conversion of magnetic energy, such as transformers, magnetic valves, sensors, and electric motors. It is worth mentioning that these materials have high magnetic scalability, allowing for high levels of magnetic strength in small volumes of the material. Moreover, their low magnetic saturation makes them efficient in responding to external magnetic fields.

Nickel-Iron (Fe-Ni) Compounds are some potential future applications :

Electronics and Semiconductors (Developing magnetic transistors to enhance performance in microelectronics), Energy Technologies and Magnetic Conversion (Producing high-efficiency transformers, thanks to their ability to reduce magnetic energy loss during conversion processes), Magnetic Sensors and Detection Devices (Developing speed and acceleration measurement devices, which rely on detecting magnetic changes in moving machinery and equipment), Medical and Biological Applications (Using Fe-Ni compounds in magnetic resonance imaging (MRI) to improve image quality and reduce magnetic noise).

REFERENCES

[1] T. Osaka, Recent development of Magnetic recording head core materials by plating method. Electrochimica Acta **44** (21-22), 3885-3890 (1999).
DOI: https://doi.org/10.1016/S0013-4686(99)00095-X

[2] H. Yang, et al., Monodisperse water-soluble Fe–Ni nanoparticles for magnetic resonance imaging. Journal of Alloys and Compounds **509** (4), 1217-1221(2011).
DOI: https://doi.org/10.1016/j.jallcom.2010.09.191

[3] M. Butta, et al., Electroplated FeNi ring cores for fluxgates with field induced radial anisotropy. Journal of Applied Physics **117** (17), 17A722 (2015). DOI: https://doi.org/10.1063/1.4914874

[4] H. Chen, et al., Template-free formation of urchin-like FeNi3 microstructures by hydrothermal reduction. Materials Letters **91**, 75-77 (2013).
DOI: https://doi.org/10.1016/j.matlet.2012.09.040

[5] C. Lei, et al., Fabrication of a solenoid-type inductor with Fe-based soft magnetic core. Journal of Magnetism and Magnetic Materials **308** (2), 284-288 (2007).
DOI: https://doi.org/10.1016/j.jmmm.2005.12.014

[6] F. Baira, et al., Calculation by Density functional theory of FeNi-2Mo and FeNi2Nd. Neuro Quantology **21** (6), 1371-1378 (2023).
DOI: https://doi.org/10.48047/nq.2023.21.6.nq23139

[7] X.-M. Zhou, X.-W. Wei, Single crystalline FeNi3 dendrites: large scale synthesis, formation mechanism, and magnetic properties. Crystal Growth and Design. **9** (1), 7-12 (2009).

[8] R. Balachandran, H.K. Yow, B.H. Ong, K.B. Tan, K. Anuar, H.Y. Wong, Surface morphology and electrical properties of pulse electrodeposition of NiFe films on copper substrates in ultrasonic field. Int. J. Electrochem. Sci. **6**, 3564-3579 (2011).
DOI: https://doi.org/10.1016/S1452-3981(23)18272-1

[9] W. Tang, K. Xu, P. Wang, X. Li, Surface roughness and resistivity of Au film on Si-(111) substrate. Microelectron. Eng. **66**, 445-450 (2003).
DOI: https://doi.org/10.1016/S0167-9317(02)00909-7

[10] G. Choe, M. Steinback, Surface roughness effects on magnetoresistive and magnetic properties of NiFe thin films. J. Appl. Phys. **85**, 5777-5779 (1999).
DOI: https://doi.org/10.1063/1.370123

[11] W. Bruckner, J. Thomas, C.M. Schneider, Evolution of stress and microstructure in NiFe thin films during annealing. Thin Solid Films **385**, 225-229 (2001).
DOI: https://doi.org//10.1063/1.370123

[12] M. Haruta, When, Gold Is Not Noble: Catalysis by Nanoparticles. Chem. Rec. **3** (2), 75-87 (2003).
DOI: https://doi.org/10.1002/tcr.10053

[13] M. Nirouei, A. Jafari, K. Boustani, Magnetic and structural study of FeNi 3 nanoparticles: effect of calcination temperature. Journal of Superconductivity and Novel Magnetism **27**, 2803-2811 (2014).
DOI: https://doi.org/10.1007/s10948-014-2727-5

[14] G. Hongxia, et al., Shape-controlled synthesis of FeNi3 nanoparticles by ambient chemical reduction and their magnetic properties. Journal of Materials Research. **27** (11), 1522-1530 (2012).
DOI: https://doi.org/10.1557/jmr.2012.67

[15] C. Zhu, et al., Nitrogen-doped carbon onions encapsulating metal alloys as efficient and stable catalysts for dye-sensitized solar cells. Journal of Power Sources **30**, 159-167 (2016).
DOI: https://doi.org/10.1016/j.jpowsour.2015.10.111

[16] Oxford university press, Physical properties of crystals: their representation by tensors and matrices. 1985 J.F. Nye.

[17] F. Baira, S. Zidani, Electronic and optical properties of ZnO: first principale investigations. Tob Regul Sci. **9** (1), 3654-3662 (2023).
DOI: https://doi.org/10.18001/TRS.9.1.256

[18] L. Tuan, T.V. Hoan, N.V. Duy, Zero-magnetization FeNi2Mo alloy: An ab initio simulation result. Computational Materials Science **180**, 109715 (2020).
DOI: https://doi.org/10.1016/j.commatsci.2020.109715

[19] Y.Mishin, M. Mehl, D. Papaconstantopoulos, Phase stability in the Fe–Ni system: Investigation by first-principles calculations and atomistic simulations. Acta Materialia **53** (15), 4029-4041 (2005). DOI: https://doi.org/10.1016/j.actamat.2024.119667

[20] A handbook. Single Crystal Elastic Constants and Caluculated Aggregate Properties. G. Simmons, 1971.

[21] H. Lu, et al., Electron work function – a promising guiding parameter for material design. Scientific Reports **6** (1), 24366 (2016). DOI: https://doi.org/10.1038/srep24366

[22] G. Wang, et al., Ab initio investigation of the elastic properties of Ni 3 Fe. Physical Review B. **88** (17), 174205 (2013). DOI: https://doi.org/10.1103/physrevb.88.174205

[23] C. Wu, B.-J. Lee, X. Su, Modified embedded-atom interatomic potential for Fe-Ni, Cr-Ni and Fe-Cr-Ni systems. Calphad. **57** 98-106 (2017). DOI: https://doi.org/10.1016/j.calphad.2017.03.007

[24] B. Holm, et al., Elastic and optical properties of α-and κ−Al2O3. Physical Review B, **59** (20), 12777 (1999). DOI: https://doi.org/10.1103/PhysRevB.59.12777

[25] Cambridge University Press On the stability of crystal lattices. I. in Mathematical Proceedings of the Cambridge Philosophical Society1940.M. Born.

[26] F. Mouhat, F.-X. Coudert, Necessary and sufficient elastic stability conditions in various crystal systems. Physical Review B. **90** (22), 224104 (2014). DOI: https://doi.org/10.1103/physrevb.90.224104

[27] J.P. Watt, L. Peselnick, Clarification of the Hashin-Shtrikman bounds on the effective elastic moduli of polycrystals with hexagonal, trigonal, and tetragonal symmetries. Journal of Applied Physics **51** (3), 1525-1531 (1980). DOI: https://doi.org/10.1063/1.327804

[28] IOP Publishing. in Journal of Physics: Conference Series. Investigation on properties of FeNi intermetallics under pressure by First-principles. 2020. M. Wang, G. Zhang, and H. Xu.

[29] G.N. Greaves, et al., Poisson's ratio and modern materials. Nature Materials **10** (11), 823-837 (2011).

[30] Haines, J., Leger, G. Bocquillon. Annu. Rev. Mater. Res. **31** (1), 1-23 (2001).

[31] S. Pugh, XCII. Relations between the elastic moduli and the plastic properties of polycrystalline pure metals. The London, Edinburgh, and Dublin Philosophical Magazine and Journal of Science **45** (367), 823-843 (1954).

[32] Y. Benkrima, et al., Comparison of the Optical Properties of Pure and Doped Iron-Nickel Alloys. Indian Journal of Pure & Applied Physics **62**, 570-575 (2024). DOI: https://doi.org/10.56042/ijpap.v62i7.8291